Molecular Interaction Model for the C1B Domain of Protein Kinase C-γ in the Complex with Its Activator Phorbol-12-myristate-13-acetate in Water Solution and Lipid Bilayer

Jozef Hritz,[†] Jozef Ulicny,[†] Aatto Laaksonen,[‡] Daniel Jancura,[†] and Pavol Miskovsky*[,†,§]

Department of Biophysics, P. J. Safárik University, Jesenná 5, 041 54 Kosice, Slovak Republic, Division of Physical Chemistry, Arrhenius Laboratory, Stockholm University, SE-106 91 Stockholm, Sweden, and International Laser Centre, Ilkovicova 3, 812 19 Bratislava, Slovak Republic

Received March 18, 2004

Detailed molecular models of the free C1B domain of protein kinase C-γ (PKC-γ) and the C1B domain with its activator phorbol-12-myristate-13-acetate (PMA) in water solution and in the presence of dipalmitoylphosphatidylcholine (DPPC) bilayer are presented. Molecular dynamics of the free C1B domain reveals hydrogen bonds, which are critical for the forming of the diacylglycerols/phorbol esters binding site, and indicates the important role of Gln27 for the geometry of this site. According to the model, PMA interacts with the C1B domain by hydrophobic interactions with Pro11 and Tyr22 and by three persistent hydrogen bonds between the C3 carbonyl group of PMA and Gly23 and between the C20 hydroxyl group of PMA and the Leu21 and Thr12 residues of the C1B domain. The C9 hydroxyl group of PMA does not interact with the C1B domain, but it is involved in the interaction with the DPPC bilayer. Two preferential orientations of the C1B−PMA complex toward the DPPC bilayer resulted from our molecular modeling study.

Introduction

Protein kinase C (PKC) is a family of serine/threonine kinases that plays a central role in cell proliferation, differentiation, and apoptosis.[1−7] The PKC isozymes are, depending on their structure and type of regulation, categorized into three groups: (i) conventional PKCs (α, βI, βII, γ), which are regulated by diacylglycerol (DAG), phospholipids and Ca^{2+}; (ii) novel PKCs (δ, ϵ, η, θ, μ), which are regulated by DAG and phospholipids; and (iii) atypical PKCs (ζ, λ), the regulation of which has not been clearly established yet. The structure of all PKCs is composed of an N-terminal regulatory region, which consists of a pseudosubstrate region and C1 and C2 domains (atypical PKCs lack the C2 domain), and a C-terminal catalytic region, which contains the C3 and C4 domains.

C1 domains in the conventional and novel PKCs are highly homologous and consist of a tandem repeat of two zinc-finger cystein-rich motifs (C1A, C1B). These subdomains are the binding sites for the PKC activator DAG and for its functional analogues phorbol esters, which compete with DAG for the same binding site and some of them can activate PKC with an affinity at least 3 orders of magnitude higher than that of DAG.[1,8,9]

The structures of various phorbol esters [e.g. phorbol-12-myristate-13-acetate (PMA), phorbol-12,13-dibutyrate (PDBU), and phorbol-13-acetate] differ only in their hydrophobic side chains at positions 12 and 13 (Figure 1). It was assumed that these hydrophobic side chains of phorbols do not alter the binding mode of phorbol esters to PKC; they only change binding affinities. Therefore, our molecular model of the interaction of phorbol-12-myristate-13-acetate (PMA) with C1B domain in water solution should represent a binding mode of a number of phorbol esters with regulatory domains of PKC.

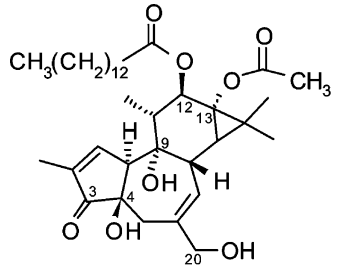

Figure 1. Structure of phorbol-12-myristate-13-acetate (PMA).

The X-ray crystallographic structure of the free C1B domain of PKC-δ and the complex of this domain with phorbol-13-acetate were determined by Zhang et al.[10] Also NMR-derived solution structures of the PKC-α C1B domain[11,12] and the PKC-γ C1B domain[13] have been reported. These analyses showed that the C1B domain consists of two antiparallel β sheets and a short helical segment, which packs against one of the sheets. Two zinc centers are present at the either end of this sheet, and each zinc atom is coordinated by three Cys and one His residues.[14,15]

The X-ray structure of Zhang[10] and the NMR structure of Hommel[11] have been frequently used as a structural basis for molecular modeling of the interactions of the C1B domain with its potent ligands.[16−19] However, these structures of the C1B domain differ significantly at the C-terminus and in the segments inside and around the second and third β strands, i.e., inside the region of the phorbol ester binding site. The molecular model of interaction between the phorbol-

* To whom correspondence should be addressed. Phone: +421 55 6222986. Fax: +421 55 6222124. E-mail: misko@kosice.upjs.sk.
† P. J. Safárik University.
‡ Stockholm University.
§ International Laser Centre.

10.1021/jm049786s CCC: $27.50
Published on Web 11/13/2004

12,13-dibutyrate (PDBU) and the C1B domain,[16] whose structure was derived on the basis of NMR experiment,[11] has a different binding mode than that observed in the X-ray-determined structure for the complex formed between the phorbol-13-acetate and the C1B domain of PKC-δ.[10] It is important to note that molecular modeling of the complex C1B−PDBU,[19] starting from the X-ray structure of the free C1B domain of PKC-δ led to the same binding mode as was seen in the X-ray structure of the complex between the C1B domain and the phorbol-13-acetate of PKC-δ.[10] The origin of the different binding modes observed in the molecular models of the C1B domain and phorbol esters can be attributed to the different loop geometry of the binding site in the X-ray and NMR structures.

More recently, the solution structure of the C1B domain of PKC-γ was determined by Xu et al.,[13] where a complete chemical shift assignment of ^{13}C, ^{15}N, and ^{1}H of the C1B domain of PKC-γ has been accomplished by heteronuclear multidimensional NMR. A well-defined core of the C1B domain (region 100−153) has been determined to a high resolution by 4D NOESY and coupling constant measurements.[13] This approach led to the more precise determination of the C1B domain structure in comparison with the Hommel NMR structure,[11] especially in the binding site region. The critical hydrogen bonds are different in these NMR structures; however, the X-ray structure reveals the same critical hydrogen bonds as Xu et al.'s NMR structure. In our view, this structure represents the most convenient starting point for molecular modeling of the free C1B domain as well as for modeling of complexes of this domain with various ligands in water solution. This structure is used in the presented paper with the purpose to obtain an improved molecular model of the free C1B domain, which in the next step was used for molecular modeling of the interaction of the phorbol-12-myristate-13-acetate (PMA) with the C1B domain in water solution.

PKC is activated by its translocation to cellular membranes, which is mediated by the embedment of regulatory domains C1 (composed of C1A and C1B) and C2 on the membrane, providing the energy to release an autoinhibitory pseudosubstrate sequence from the active site of PKC.[20] The interaction of the C1B domain with membranes is driven by three known mechanisms: by binding diacyglycerols or phorbol esters, by a nonspecific electrostatic interaction with anionic lipids, and by stereoselective interaction with phosphatidylserine. This interaction is insensitive to physiological Ca^{2+}. The interaction of the C2 domain is driven by binding Ca^{2+} and by a nonspecific electrostatic interaction with anionic lipids.[20,21] The analysis of binding of PKC to membrane showed that the interaction of PKC with phorbol esters is so strong that PMA is able to recruit PKC to neutral phosphatidylcholine membranes in the complete absence of acidic lipids.[22,23]

Johnson et al. showed that the isolated C1B domain binds neutral membranes composed of phosphatidylcholine in a phorbol ester dependent manner and moreover found that the binding affinity of the C1B domain to neutral membranes containing PMA is similar to that of full-length protein. The similarity in binding constants reveals that the domain is equally accessible to neutral membranes alone or in the context of full-length protein.[21] Taking into account the additional facts that the C2 domain is insensitive to diacylglycerol and phorbol esters as well as that C2 domain does not bind the neutral lipids[21] led us to the suggestion that the molecular model of the interaction of C1B domain with PMA incorporated in phosphatidylcholine bilayer (the C1B−PMA−DPPC complex) will represent activation of PKC by PMA in the presence of the neutral phosphatidylcholine membrane.

An overwhelming majority of molecular modeling studies of membranes were performed using neutral zwitterionic phospatidylcholines. The DPPC bilayer is usually used as the membrane model, due to the best developed methodology of molecular dynamics simulation of DPPC bilayer in comparison with other phospholipids bilayers. Only a few molecular dynamics studies of negatively charged lipid bilayers have been reported.[24,25] There are still difficulties in treatment of strong electrostatic interactions and there is lack of experimental data that can be used for proper fitting of simulation parameters. Molecular dynamics simulations investigating protein/lipids systems used almost exclusively phosphatidylcholine bilayers as membrane model.[26−32] These are the main reasons why DPPC was chosen for our study, despite the well-known biological importance of negatively charged phosphatidylserines for activation of PKC. Moreover, the studied system (C1B−PMA−DPPC complex) is not out of biological relevance, because the isolated C1B binds to neutral phosphatidylcholine membrane containing PMA.[21]

Experimental Section

The Structure of the C1B domain of PKC. The NMR-determined structure of the C1B domain of PKC-γ in water solution[13] was taken from the Brookhaven Protein Data Bank[33] (filenames: 1TBN, energy minimized average structure; 1TBO, 30 refined simulated annealing structures). Only the core of the C1B domain is required for binding of ligands (e.g. phorbol esters).[34] We used this core region extended by two amino acids (region 99−154) in our molecular modeling study. The extension was carried out to avoid artificial electrostatic interactions between the edges of peptide with Zn^{2+} cations. To facilitate comparison of our molecular model with the previous one[16] and the X-ray structure,[10] we preserved the same numbering scheme of residues of the C1B domain. For the peptide, the extended-atom GROMOS-87 force field[35,36] was used, as implemented in the GROMACS MD simulation package.[37,38] The water was modeled as standard SPC.[39] When necessary, Na^+ and Cl^- counterions were added to electroneutralize the whole system.

The crystal coordinates of the C1B domain of PKC-δ (code 1PTQ) when free and in the complex with phorbol-13-acetate (1PTR)[10] were retrieved from the Brookhaven Protein Data Bank.

Phorbol-13-acetate and Phorbol-12-myristate-13-acetate Structures

The 3D structure of phorbol-13-acetate was taken from the crystal structure of the C1B domain of PKC-δ in complex with phorbol-13-acetate (1PTR)[10] and was used for ab initio quantum mechanical calculations of energetically optimized structure and charge distribution using the Merz−Kollman scheme (Gaussian 98, B3LYP/6-31G*). The 3D structure of phorbol-12-myristate-13-acetate was constructed by attaching the myristate chain to phorbol-13-acetate at position 12 (Figure 1).

Structure of Dipalmitoylphosphatidylcholine Bilayer. The lipid system is represented by 64 DPPC molecules, arranged in a bilayer conformation, and 3476 water molecules, forming a large layer (approximately 6.1 nm). The inclusion

of a large water layer was required to eliminate the problem of artificial interaction between the C1B domain with the periodic image of the bilayer. As an initial structure of DPPC bilayer, the last frame of the 60 ns trajectory generated by Lindahl et al.[40] was used. This bilayer can be considered well-equilibrated. The force field and simulation parameters for a DPPC bilayer at full hydration have been described in detail[41] and shown to accurately reproduce experimental quantities such as the volume/lipid[42] and order parameters.[43] GROMOS-87[35,36] united atom types were used for the CH_2/CH_3 groups in the hydrocarbon tails, reducing the number of atoms per lipid to 50. Atomic charges were taken from ab initio quantum mechanical calculations.[44] For the DPPC hydrophilic headgroup the Lennard-Jones parameters were taken from the optimized potentials for liquid simulations force field,[45] while for the hydrophobic tail, parameters determined by Berger et al.[41] were used. Bond rotations in the carbon tails were modeled with Ryckaert−Bellemans dihedrals[46] and the corresponding 1,4-interactions were removed. For the myristate tail of PMA, the same force field parameters as for hydrophobic tails of DPPC were used.

Molecular Modeling. All molecular dynamics simulations were carried out using the Gromacs MD simulation package (version 3.1.4) running on a Linux cluster. The Verlet integration scheme[47] (leapfrog) was used with a time step of 2 fs. Periodic boundary conditions with a rectangular box were applied to avoid edge effects. The LINCS algorithm[48] was used to constrain all covalent bonds in non-water molecules. The SETTLE algorithm[49] was used to constrain the bond lengths and angles in the water molecules. The temperature was controlled by using a weak coupling to a bath[50] of 300 K in the complex without the lipid bilayer and of 323 K in the system containing DPPC bilayer, well above the phase transition at 315 K with a time constant of 0.1 ps. Solvent (i.e. water and counterions), protein, and lipids were independently coupled to the heat bath. Initial velocities were randomly generated from the Maxwell distribution at 300 K, according to atomic masses. The pressure was also controlled using weak coupling[50] to atmospheric pressure with a time constant of 1.0 ps. For the system without lipid bilayer, isotropic scaling was used. For the system containing the DPPC bilayer, a separate scaling to atmospheric pressure in lateral and normal directions, which produce an average zero surface tension, was used. The van der Waals interactions were modeled using a 6−12 Lennard-Jones potential, with cutoff at 14 Å. Long-range electrostatic was treated by the particle mesh Ewald algorithm,[51] with a 9 Å cutoff for the direct space interactions, and the reciprocal space interactions were evaluated on a 0.12 nm grid with the fourth-order spline interpolation. The reciprocal space calculation was performed using a fast Fourier transformation algorithm. Molecular dynamic trajectories as well as static structures were visualized using VMD molecular visualizer[52] and POV-Ray renderer.[53] Secondary structure analysis of protein was done using the DSSP program.[54]

Results and Discussion

Molecular Model of C1B Domain. Molecular dynamics simulations were performed to investigate the stability and flexibility of our model of the C1B domain (Figure 2), based on the NMR-determined energy-minimized average structure of the core region of the C1B domain (for details see the Experimental Section).[13] The rmsd analysis of the 1 ns molecular dynamics trajectory of this model in water solution at room temperature showed that the initial NMR structure is sufficiently stabilized after 50 ps (Figure 3). Secondary structure analysis of the molecular dynamics trajectory showed that the regions 3−6, 12−14, 19−21, 28−31, and 36−37 form the β strands and region 42−45 forms the α helix during almost the whole time of simulation. The averaged rmsd of the backbone part of each amino acid of the C1B domain is shown in the Figure 4. The shape

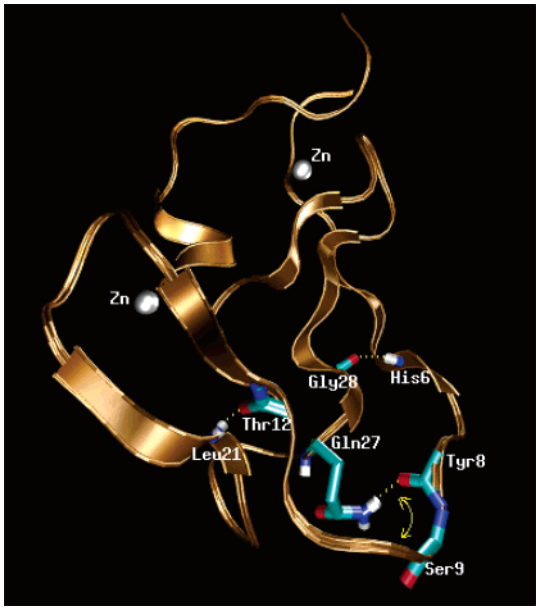

Figure 2. Molecular model of the C1B domain of PKC-γ in ribbon representation. Hydrogen bonds critical for the forming of the binding site are shown as dashed yellow lines.

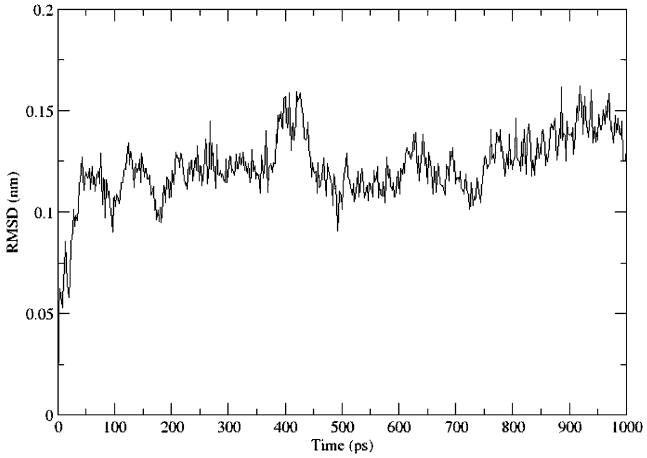

Figure 3. Time evolution of the rmsd of the backbone of the free C1B domain in water solution.

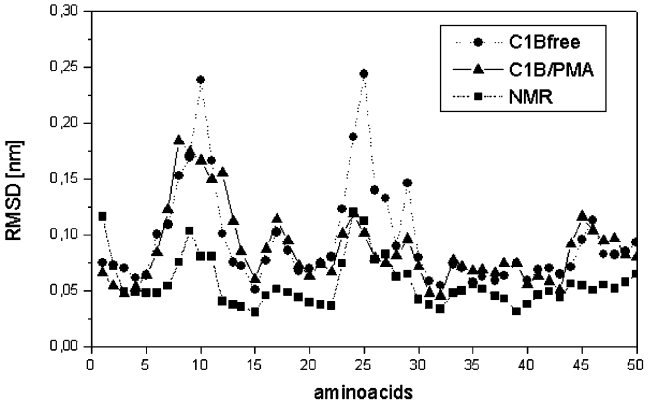

Figure 4. Rmsd of the backbone by residue from molecular dynamics of the free C1B domain, of the C1B domain in the complex with PMA, and from 30 NMR-derived solution structures.[13]

of the obtained rmsd function is in quite good agreement with the same rmsd analysis within the ensemble of 30 NMR structures.[13] As can be seen from Figure 4, the regions 6−14 and 23−29, where DAG/PE binding site

is localized, have a high degree of flexibility. The flexibility of both of the mentioned regions is a source of problem for precise NMR analysis of the structure of this region. In such cases, MD represents a very useful tool for describing dynamic aspects and revealing the hydrogen-bond network of these highly flexible structures. The knowledge of the hydrogen-bond network in this region is necessary for the precise determination of the geometry of the binding site.

Molecular dynamics simulations allow us to determine the average residence time of hydrogen bonds, reflecting their stability. The average residence time presents the percentual fraction of existence of the hydrogen bond out of the total time of simulation. In the following text, we will report these residence times in parentheses after description of each individual hydrogen bond.

Molecular dynamics simulations reveal that there are two critical hydrogen bonds, determining the length of the loops forming the binding site. The first one is between the carbonyl group of Thr12 and the NH group of Leu21 (95%) and the second one is between the backbone NH group of His6 and the carbonyl group of Gly28 (89%) (Figure 2).

Wang et al.[16] determined the critical hydrogen bonds in an NMR solution structure of the C1B domain of PKC-α solved by Hommel[11] as well as in the X-ray structure of the C1B domain of PKC-δ.[10] For the NMR structure he proposed hydrogen bonds between NH of Thr12 and the carbonyl of Leu21 and between the NH of Tyr8 and the carbonyl of His26. For the X-ray structure he determined the first hydrogen bond between the carbonyl of Thr12 and the NH of Leu21 and the second one between the carbonyl of Tyr6 and the backbone NH of Gln27. As was pointed out, these differences lead to a different geometry of the binding site and consequently to different binding modes for the ligands.[16]

However, our analysis of the critical hydrogen bonds in the same X-ray structure of the C1B domain of PKC-δ[10] showed the same first hydrogen bond, but instead of the second one, we found a hydrogen bond between NH of Tyr6 and the carbonyl of Gly28. In our opinion, the hydrogen bond determined by Wang et al. between the carbonyl of Tyr6 and the backbone NH of Gln27 is unlikely, due to very unfavorable relative orientation of these residues, despite quite close distance of heavy atoms. The same hydrogen bonds constraining the binding site, coming out from our analysis of the X-ray structure of the C1B domain, are observed also in our model of the C1B domain. Thus, we can conclude that the refined hydrogen-bond model based on our MD simulations (Figure 2) is compatible with both the X-ray data[10] and the NMR data.[13]

We would like also to emphasize that according to the presented model, the binding site geometry is affected by the side chain of Gln27, which modifies the original NMR solution structure of the free C1B domain proposed by Xu.[13] Our model reveals that the carbonyl group and backbone NH group of Gln27 form an intraresidual hydrogen bond (68%). Moreover, the NH_2 group of the Gln27 side chain forms a hydrogen bond with the carbonyl of Tyr8 (43%) and/or the carbonyl of Ser9 (28%) (Figure 2). These alternating hydrogen bonds effectively connect two loops, which form the DAG/PE binding site and thus significantly contribute to the geometry of this site. The mutational experiments proved the importance of Gln at position 27.[19] Mutations Gln27 → Gly and Gln27 → Trp led to a complete loss of the binding of PDBU to the C1B domain. We would like to mention that this observation is difficult to explain within the ensemble of the 30 NMR structures determined by Xu et al.,[13] where the position of the Gln27 side chain is very flexible and the above-mentioned hydrogen bonds of the NH_2 group of Gln27 are present only in three structures out of the total thirty. In fact, the NMR experiment revealed only one NOE distance about Gln27, so there exists a high uncertainty concerning the geometry of the Gln27 residue. Our suggestion about the geometry of the Gln27 side chain is also supported by X-ray data.[10] According to the X-ray structure, there are two possibilities for the hydrogen bond involving the carbonyl group of the Gln27 side chain: the first one with the backbone NH group of Gln27 (present in our model) or the second one with the backbone NH group of Tyr8. For the NH_2 group of Gln27 side chain, there are three possibilities for hydrogen bond interactions: with the carbonyl of Tyr8 (present in our model), with the carbonyl of Gly 23, or with the carbonyl of Leu24.

To summarize, our molecular model of the free C1B domain, based on the NMR structure of the C1B domain determined by Xu et al.[13] with corrected Gln27 side-chain position, improves the molecular model of the free C1B domain with a more precise geometry for the phorbol binding site. We consider this model as the most advisable starting point for obtaining solution structural models of interaction of the C1B domain with various ligands. This model was used in the following simulations of the interaction of the C1B domain with the PMA and DPPC bilayer.

Molecular Model of the C1B−PMA Complex. For molecular modeling of the C1B−PMA complex, the PMA molecule was positioned into the entrance of the binding site of the C1B domain, and 10 independent simulated annealing runs (with different starting PMA positions) were carried out for 2 ns. The analysis of these simulations showed that for 8 out of 10 final structures the same binding mode was found (Figure 5). In this binding mode, the position of PMA in the complex with the C1B domain is stabilized by hydrophobic interactions of Pro11 with the seven-member ring of PMA and of Tyr22 with the five-member ring of PMA, and four hydrogen bonds between PMA and C1B domain are formed: the C3 carbonyl group interacts with the NH group of Gly 23 (84%), the hydroxyl group at C20 acts as the hydrogen bond donor to the carbonyl oxygen of Leu 21 (98%) and as the hydrogen bond acceptor in the interaction with the NH group of Thr 12 (93%), and a weaker hydrogen bond is formed between the carbonyl oxygen of the ester at C13 and the hydroxyl group of Ser 10 (37%) (Figure 5).

The 2 ns molecular dynamics simulations of the obtained C1B−PMA complex were performed. The rmsd analysis (Figure 4) showed that the flexibility of the loop region 24−31 was significantly decreased, while the flexibility of the other loop is changed only slightly. The secondary structure analysis of this run shows that the structure of the C1B domain is nearly unchanged after binding to PMA. Analysis of the average hydrogen-bond

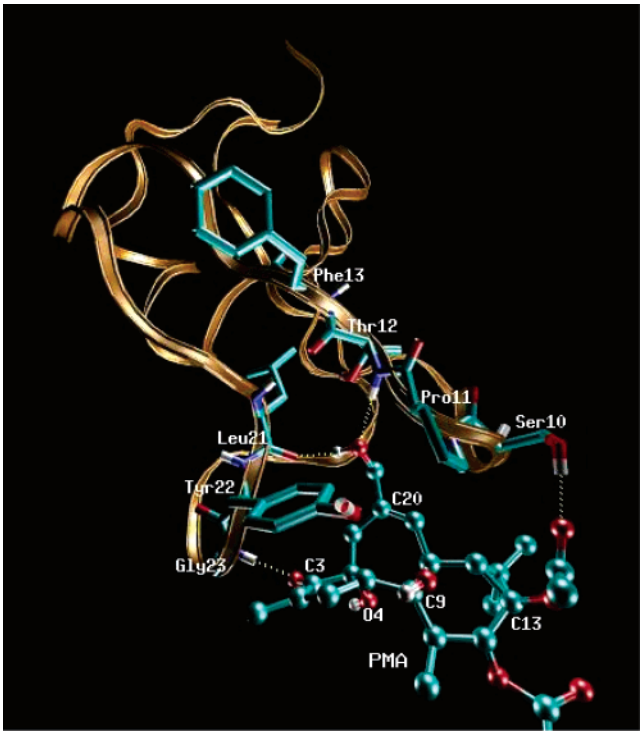

Figure 5. Molecular model of the C1B domain of PKC-γ in the complex with PMA in ribbon representation. Amino acids interacting with PMA are shown explicitly. Hydrogen bonds critical for forming of the binding site are shown as dashed yellow lines.

residence times shows that hydrogen bonds within the C1B domain are only slightly changed upon the interaction with PMA. The hydrogen bonds between PMA and Gly23, Leu21, and Thr12 of the C1B domain are very stable during almost the entire simulation. The carbonyl oxygen of the ester at C13 as hydrogen-bond acceptor alternates in two hydrogen bonds; for 37% of simulation time it interacts with hydroxyl group of Ser10, while for 42% of simulation time it forms an intramolecular hydrogen bond with the C9 hydroxyl group of PMA.

This intramolecular hydrogen bond as well as the above-mentioned three most persistent intermolecular hydrogen bonds between PMA and Gly23, Leu21, and Thr12 of the C1B domain are clearly observed in the X-ray structure of the phorbol-13-acetate−C1B domain complex.[10] The hydrogen bond between the carbonyl oxygen of the ester at C13 and the hydroxyl group of Ser10 was not observed in the X-ray structure. The reason is that this hydrogen bond alternates with the more dominant intramolecular hydrogen bond between the hydroxyl group at C9 and the carbonyl oxygen of the ester at C13 (present in the X-ray structure). The existence of the hydrogen bond between the carbonyl oxygen of the ester at C13 and the hydroxyl group of Ser10 in the presented molecular model is supported by binding affinity measurements of phorbol analogues to PKC, where it was shown that in addition to the three oxygen functional groups at C3, C9, and C20, the C13-ester group is strongly implicated as important in PKC−ligand interactions.[55,56] On the other side, hydrogen bond between the C4 hydroxyl group of PMA and the carbonyl group of Gly23 as observed in the X-ray model is not present in our simulation. The reason for this discrepancy can be attributed to the different phase of the studied objects. Our model represents the complex of the C1B domain with PMA in solution, while Zhang et al. studied the crystal of this complex.[10] Thus, our model provides an explanation to the experimental finding that the C4 hydroxyl group of phorbol esters is not necessary for PKC binding in solution.[57] We can confirm the conclusion from the work of Tanaka et al.[57] that the X-ray structure of the C1B domain might not adequately reflect the true interaction in solution between phorbol esters and PKC.

The model presented here is also in a very good agreement with the NMR experiment,[13] where it was found that the binding of the phorbol ester affected the NMR signal of Ser10, Thr12, Phe13, Leu21, Tyr22, and Gly23. The origin of these changes can be naturally explained by our model, in which PMA interacts with Ser10, Thr12, Leu21, and Gly23 via hydrogen bonds (Figure 5). The side chain of Tyr22 is moved after binding of PMA. However, our model does not give a clue for the origin of the shift of the NMR signal of Phe13, but it can be affected by the strong change in the hydrophobicity of the environment after binding of PMA.

In the previously proposed molecular model of the complex of the C1B domain with PDBU in water solution,[16] the oxygen of the C3 carbonyl group of PDBU forms hydrogen bonds with the backbone NH groups of Ile25 and His26 and a weaker hydrogen bond with the NH of Gly28. The C20 hydroxyl group, as a hydrogen-bond acceptor, binds to the NH groups of Tyr8 and Gly9 and acts as a hydrogen-bond donor with either the carbonyl group of Ser10 or the side chain hydroxyl of Thr12. The hydroxyl group at C9 of PDBU forms a weak hydrogen bond with the NH of Thr12 and a strong intramolecular hydrogen bond with the carbonyl group of the ester at C13 of the PDBU. The oxygen of this group forms a strong hydrogen bond with the NH of Thr12. The carbonyl group at C12 is exposed to solvent and is without significant interactions with the protein during the simulations. According to the model of Wang et al.,[16] there is only a minor interaction between the C4 hydroxyl group of PDBU and the C1B domain. From the Wang molecular model,[16] it follows that the amino acids of the C1B domain interacting by hydrogen bonds with PDBU are Ile25, His26, Gly28, Tyr8, Gly9, Ser10, and Thr12. However, the NMR signal is only affected for two of them (Ser10 and Thr12) after the PDBU binding. Disagreement between the Wang model and NMR experiment is also observed in the NMR signal of Ph13, Leu21, Tyr22, and Gly23, where the molecular model gives no reason to expect experimentally observed signal broadening. There are also discrepancies between the Wang model[16] and the X-ray data,[10] which have been already described.[16] The above mentioned arguments raise questions about the correctness of the Wang molecular model. As was shown above, our model nicely correlates with both the X-ray and the NMR data and therefore should considered as a more precise model of interaction of phorbol esters with the C1B domain of PKCs.

Whereas our interaction model of PMA with the C1B domain leads to the same binding mode as observed in the X-ray and the NMR experiments for the phorbol-13-acetate and the phorbol 12,13-dibutyrate, it also adds

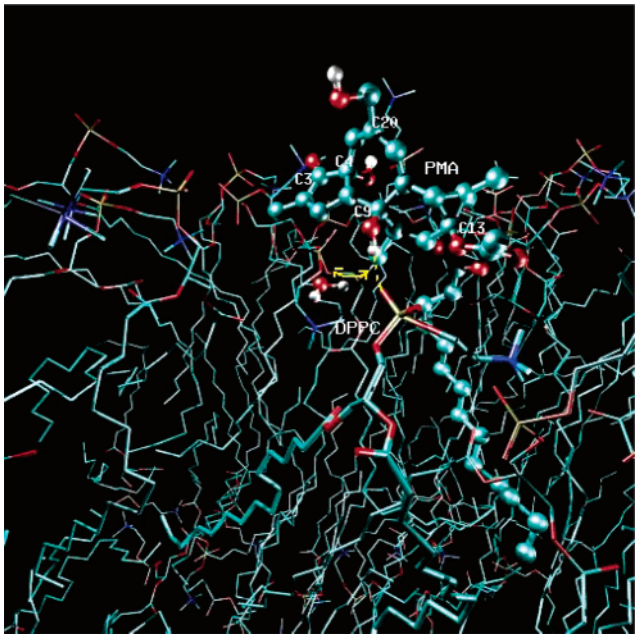

Figure 6. Molecular model of PMA incorporated in the DPPC bilayer. The hydrogen bond involving C9 hydroxyl group of PMA is showed as a dashed yellow line.

weight to the already presented view that the binding mode of phorbol esters is not affected by the lengths of the esteric parts and that the esteric part modulates only the binding affinity.[19]

Interaction with Lipid Bilayer. Since the PKC is activated by a translocation to cellular membranes after DAG−phorbol binding, it can be expected that lipids may influence the structure of the complex. To investigate the influence of membrane on the structural characteristics of the C1B−PMA complex, the model of ternary complex C1B−PMA−DPPC bilayer was constructed. As a first step toward modeling of the ternary complex, we have studied the incorporation of PMA into the DPPC bilayer.

Molecular Model of Complex of PMA with DPPC Bilayer. The structure of the PMA−DPPC bilayer system with the tail of the hydrophobic chain of PMA partially incorporated into the bilayer was chosen as the initial conformation. Next, the optimal configuration of PMA with the respect to the DPPC bilayer was sought during 20 ns molecular dynamics simulations. During the first 8 ns, PMA penetrated deeper into the bilayer; after this time, its position remained practically unchanged (Figure 6). Analysis of the average residence times of the hydrogen bonds showed that the C9 hydroxyl group of PMA as hydrogen-bond donor alternates in three types of hydrogen bonds. For 32% of the simulation time, it forms a hydrogen bond with the phosphate group of DPPC molecules; for 47% a hydrogen bond is formed with water molecules in the lipid phase, which surround the headgroups of the DPPC molecules; and for 14% of simulation time, it forms intramolecular hydrogen bond with the carbonyl oxygen of the ester at C13 of PMA. Thus, our model suggests that the C9 hydroxyl group is highly involved in the interaction with the lipid bilayer. Figure 6 shows that the C3 carbonyl and the C4 and C20 hydroxyl groups of PMA interact with bulk water solution. This model of the PMA−DPPC bilayer complex, besides serving as a starting point to the molecular modeling study of the C1B−PMA complex with the DPPC bilayer, is also interesting by itself, because it represents the first known simulation of the PMA−DPPC bilayer complex.

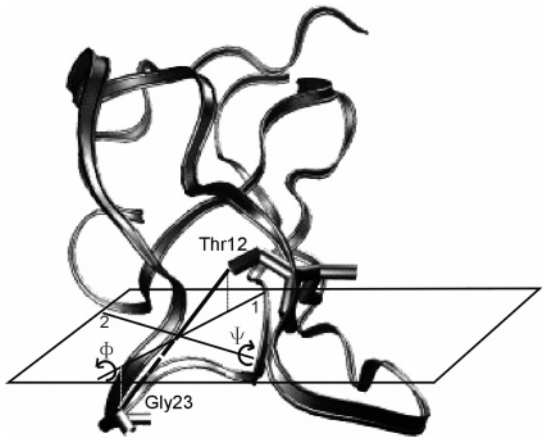

Figure 7. Schematic presentation of the rotation of the protein around axes 1 and 2. Axis 1 is a projection of a line between the NH group of Gly23 and the NH group of Thr12 to the plane passing through the midpoint of this line and parallel with the DPPC bilayer surface. Axis 2 also passes through the midpoint and is perpendicular to axis 1 in the above-mentioned plane.

Model of the C1B−PMA in the Complex with DPPC Bilayer. The construction of the molecular model of the C1B−PMA in the complex with the DPPC bilayer faces the problem of the proper orientation of the C1B domain with respect to the DPPC bilayer. Computational demand for the spontaneous orientation by standard molecular dynamics simulation exceeds our current resources; thus, we have designed an alternative approach of how to find the mutual orientation of the C1B domain and the lipid bilayer. We utilized the fact that the C1B domain interacts with the lipid bilayer in such a way that the phorbol ester binding site is oriented toward the bilayer surface.[13] With this restriction the orientation of the C1B domain toward the bilayer can be described by two degrees of freedom. Each position of the C1B domain relative to the bilayer is determined by two rotational angles around two perpendicular axes attached to the middle of the line connecting the NH group of Gly23 and NH group of Thr12. We defined the first axis as a projection of this line into the plane, parallel with the bilayer surface coming through the midpoint of the NH group of Gly23 and NH group of Thr12, and the second axis also lies on this plane and is perpendicular to the first one (Figure 7). By rotation of the C1B domain around these axes we calculated the atomic positions of 400 different orientations of C1B domain (in the interval from −50° to 50° around each axis with 5°/step; the range of sampled angles was chosen in accordance with steric constraints associated with the corresponding complex). In the next step the molecular models of C1B−PMA in the complex with DPPC bilayer were constructed for each of the above-mentioned orientations. In a vacuum we found no preferential orientation of the C1B domain toward the lipid bilayer. Thus, we expect that the preference in the orientation is due to the interaction with water, and a realistic simulation should involve water molecules. A straightforward addition of water

Table 1. Amino Acids within the C1B Domain Affected by Lipid Bilayer Presence[a]

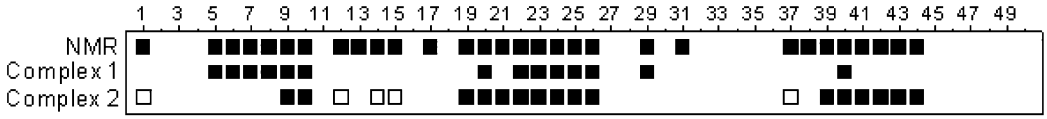

[a] Direct interactions are marked by filled squares and indirect interactions by empty squares.

molecules into these vacuum models faces the problem of a very slow relaxation. For this reason we adopted the following approach for the creation of 400 water solution molecular models of C1B−PMA in the complex with the DPPC bilayer: We used an initial structure corresponding to the orientation of 0° around the axes with equilibrated water molecules around. Models with other C1B orientations were created by a molecular dynamics procedure, during which the position restraints to the backbone atoms of the C1B domain were applied with equilibrium positions calculated by a rotation procedure. All lipid molecules, except the closest ones to PMA, were position-restrained to their initial positions. The rest of the system was without further restraints. During the described 50 ps molecular dynamics run, the C1B domain was slowly dragged to the required protein orientation. After this procedure, the position restraints to the backbone of the C1B domain were relaxed, and during the next 50 ps the complex was equilibrated. During the following 50 ps, the potential energy of such a complex was calculated every 20 fs and averaged. The analysis of such a potential energy surface showed two orientations corresponding to the most favorable interaction of the C1B domain with the lipid bilayer.

The resulting two complexes were used as starting conformations for the following 30 ns MD simulations, which led to the final molecular models of C1B−PMA in the complex with the DPPC bilayer (Figure 8A,B). The structure of the C1B domain in the C1B−PMA−DPPC complex at 325 K (the higher temperature is required for the liquid-crystal phase of the DPPC bilayer) shows higher flexibility compared to the complex C1B−PMA at 300 K, but no conformational changes of protein are observed during the time of simulation. Figure 8A,B shows that in the both models the C1B domain is partially incorporated in the DPPC bilayer. The analysis of the resulting models showed that there are 20 amino acids of the C1B domain affected by direct interaction with DPPC molecules, and at least five other amino acids are indirectly influenced through strong inter-residual interactions (Table 1). The NMR signal of *all* these 25 amino acids within the C1B domain was changed in the NMR study after the lipid micelle added to the solution of the C1B domain of PKC-γ.[13] This points out that both orientations of the C1B domain incorporated in DPPC bilayer are relevantly present in the system at room temperature. The fact that our model is able to explain the changes in at least 25 out of 30 experimentally observed affected amino acids raises our confidence in the realism of our model.

The binding mode of PMA to the C1B domain is only slightly changed by adding the DPPC bilayer. We have observed the same hydrogen bonds formed between PMA and the C1B domain as were observed in the complex without the DPPC bilayer with only one exception: the hydrogen bond between the carbonyl oxygen of the ester at C13 and the hydroxyl group of Ser10 is not present in the second of two final ternary complexes (Figure 8A). We also observe that the C9 hydroxyl group of PMA in the ternary system is involved in the interaction with the DPPC bilayer in the same manner as in the PMA−DPPC bilayer complex.

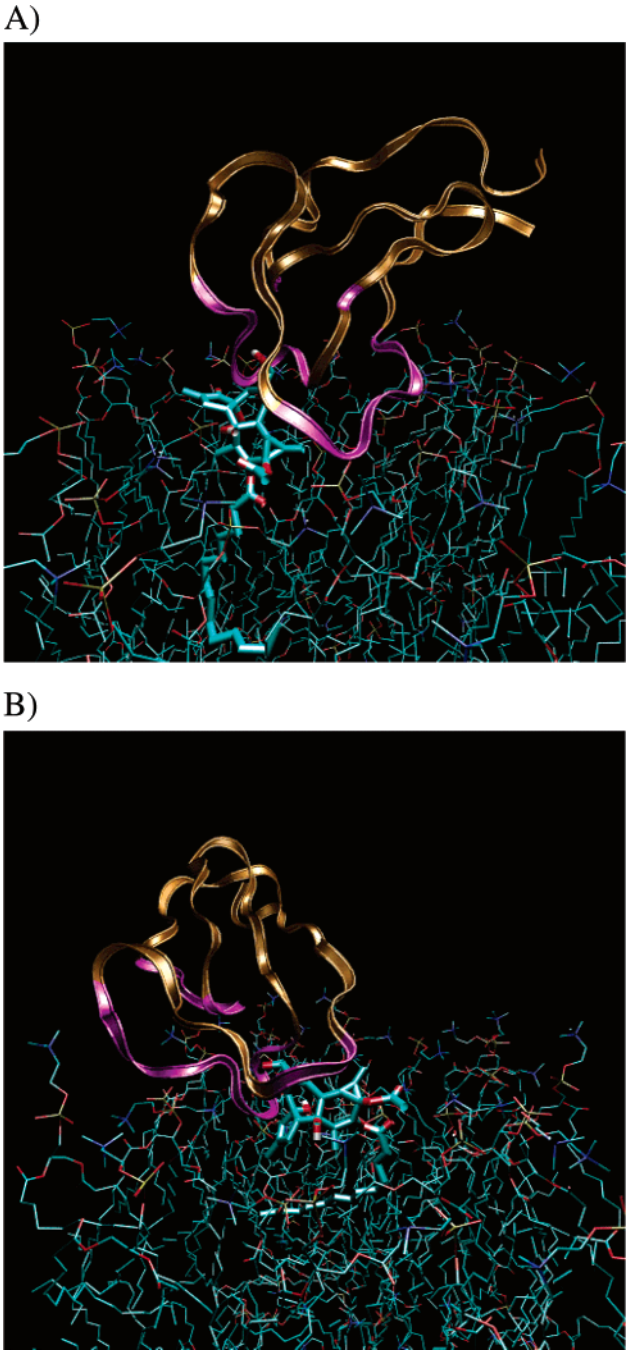

Figure 8. Molecular model of two possible orientations of the C1B−PMA complex within the DPPC bilayer. The C1B domain is drawn in ribbon representation. Parts interacting with DPPC bilayer are in purple.

Conclusions

The molecular dynamics simulation of the free C1B domain of PKC and the C1B domain with its activator phorbol-12-myristate-13-acetate (PMA) in water solution and in the presence of dipalmitoylphosphatidylcholine (DPPC) bilayer was performed. The molecular dynamics trajectories of the free C1B domain, the C1B−PMA complex, and the C1B−PMA−DPPC bilayer complex were analyzed in order to provide a detailed interaction models.

The resulting molecular mechanical model of the free C1B domain reproduces the critical hydrogen bonds constraining the length of the loops forming at the diacylglycerols/phorbol esters binding site, observed in the X-ray structure.[10] Our study emphasizes the role of Gln27 for forming of the binding site in the C1B domain, for which the NMR-based structural models, proposed by Xu et al.,[13] provide no explanation.

This improved model of the free C1B domain was used to construct the structural model of the complex of the C1B domain with PMA. In this model PMA interacts with the C1B domain by hydrophobic interactions with Pro11 and Tyr22 and by three persistent hydrogen bonds between the C3 carbonyl group of PMA and Gly23 and between the C20 hydroxyl group of PMA and Leu21 and Thr12 residues of the C1B domain. The carbonyl oxygen of the ester at C13 forms a weaker hydrogen bond with the hydroxyl group of Ser 10. This bond alternates with the intramolecular hydrogen bond between the carbonyl oxygen of the ester at C13 and the hydroxyl group at C9. The molecular dynamics simulations allow us to explore the dynamics of the hydrogen-bond system, inaccessible in the X-ray study. The resulting binding mode is very similar to the binding mode observed in the X-ray except for the C4 hydroxyl group, which is of minor significance for the binding in our model. Also a very good agreement with the NMR experiments of the interaction of the C1B domain with phorbol esters has been achieved.

A new efficient approach to sample the potential energy surface of the C1B−PMA−DPPC bilayer system in water solution was applied in this work. We found two preferential mutual orientations of the C1B−PMA complex toward the lipid bilayer. The proposed model reveals that the binding mode of PMA to the C1B domain is only slightly changed upon the addition of the DPPC bilayer. The importance of the C9 hydroxyl group of PMA for the formation of hydrogen bond with the lipid bilayer was revealed.

Johnson et al. showed that the affinity of the isolated C1B domain for PMA-containing neutral membranes composed of phosphatidylcholine is the same as that of full-length PKC.[21] Thus, it is reasonable to assume that the C1B domain within full-length PKC has the same binding mode to neutral membrane containing PMA as the isolated C1B domain in our molecular model of the C1B−PMA−DPPC complex. In the same study it is showed that the presence of phosphatidylserine increased the binding affinity of the C1B domain for PMA containing membranes by over 2 orders of magnitude.[21] Thus an improvement of methodology of simulations of charged lipid bilayers and their interactions with proteins, which can be expected in the very near future, will give us the possibility to create the molecular model of C1B−PMA incorporated to the bilayer composed of phosphatidylcholines and phosphatidylserines. Comparison of the binding mode in such a complex with the one presented in this paper would show if the presence of phosphatidylserines influence only binding affinity (observed experimentaly[21]) or also influence the binding mode of the C1B domain bound lipids bilayers containing PMA.

The presented new mechanistic models can serve as a suitable base for the ligand binding studies and rational drug design for this important class of regulatory proteins. Besides detailed structural information about the C1B−PMA−DPPC complex, our work brings also a general methodological approach that can be applied to study other surface membrane bounded proteins and to encourage many future studies devoted of this practically important class of systems.

Acknowledgment. This work forms a part of Ph.D. thesis of J.H. This work was supported by Science and Technology Assistance of Slovak Republic Agency under the contract no. APVT-20-022202 and by the Swedish Institute (5 months stay at Stockholm University for J.H.). Support from the Swedish Science Council (VR) is acknowledged.

Appendix

Abbreviations. PKC, protein kinase C; MD, molecular dynamics; DAG, 1,2-diacylglycerol; NMR, nuclear magnetic resonance; NOESY, nuclear Overhauser effect spectroscopy; PMA, phorbol-12-myristate-13-acetate; DPPC, dipalmitoylphosphatidylcholine; PDBU, phorbol 12,13-dibutyrate.

Supporting Information Available: Molecular modeling coordinates in pdb file format of the resulting structures of free C1B domain, C1B−PMA complex, PMA−DPPC complex, C1B−PMA−DPPC complex 1, C1B−PMA−DPPC complex 2. This material is available free of charge via the Internet at http://pubs.acs.org.

References

(1) Nishizuka, Y. The Role of Protein Kinase C in Cell Surface Signal Transduction and Tumor Promotion. *Nature* **1984**, *308*, 693−698.
(2) Nishizuka, Y. Studies and Perspectives of Protein Kinase C. *Science* **1986**, *233*, 305−312.
(3) Nishizuka, Y. The Molecular Heterogeneity of Protein Kinase C and Its Implications for Cellular Recognition. *Nature* **1988**, *334*, 661−665.
(4) Kikkawa, U.; Kishimoto, A.; Nishizuka, Y. The Protein Kinase C Family: Heterogeneity and Its Implication. *Annu. Rev. Biochem.* **1989**, *58*, 31−44.
(5) Lester, D. S.; Epand, R. M., Eds. *Protein Kinase C, Current Concepts and Future Perspectives;* Ellis Horword, Ltd.: New York, 1992.
(6) Clemens, M. J.; Trayner, I.; Menay, J. The Role of Protein Kinase C Isoenzymes in the Regulation of Cell Proliferation and Differentiation. *J. Cell Sci.* **1992**, *103*, 881−887.
(7) Dekker, L. V.; Parker, P. J. Protein Kinase C − a Question of Specificity. *Trends Biochem. Sci.* **1994**, *19*, 73−77.
(8) Blumberg, P. M. Protein Kinase C as the Receptor for the Phorbol Ester Tumor Promoters: Sixth Rhoads Memorial Award Lecture. *Cancer Res.* **1988**, *48*, 1−8.
(9) Ron, D.; Kazanietz, M. G. New Insights into the Regulation of Protein Kinase C and Novel Phorbol Ester Receptors. *FASEB J.* **1999**, *13*, 1658−1676.
(10) Zhang, G.; Kazanietz, M. G.; Blumberg, P. M.; Hurley, J. H. Crystal structure of the Cys2 Activator-Binding Domain of Protein Kinase C Delta in Complex with Phorbol Ester. *Cell* **1995**, *81*, 917−24.
(11) Hommel, U.; Zurini, M. Solution Structure of a Cystein Rich Domain of Rat Protein Kinase C. *Nat. Struct. Biol.* **1994**, *1*, 383−387.

(12) Ichikawa, S.; Hatanaka, H.; Takeuchi, Y.; Ohno, S.; Inagaki, F. Solution Structure of Cysteine-Rich Domain of Protein Kinase C Alpha *J. Biochem.* **1995**, *117*, 566−574.
(13) Xu, R. X.; Pawelczyk, T.; Xia, T.-H.; Brown, S. C. NMR Structure of a Protein Kinase C-γ Phorbol Binding Domain and Study of Protein Lipid Micelle Interactions. *Biochemistry* **1997**, *36*, 10709−10717.
(14) Ono, Y.; Fujii, T.; Igarashi, K.; Kuno, T.; Tanaka, C.; Kikkawa, U.; Nishizuka, Y. Phorbol Ester Binding to Protein Kinase C Requires a Cysteine-rich Zinc Fingerlike Sequence. *Proc. Natl. Acad. Sci. U.S.A.* **1989**, *86*, 3099−3103.
(15) Quest, A. F.; Bloomenthal, J.; Bardes, E. S.; Bell, R. M. The Regulatory Domain of Protein Kinase C Coordinates Four Atoms of Zinc. *J. Biol. Chem.* **1992**, *267*, 10193−10197.
(16) Wang, S.; Kazanietz, M. G.; Blumberg, P. M.; Marquez, V. E.; Milne G. W. A. Molecular Modeling and Site-Directed Mutagenesis Studies of a Phorbol Ester-Binding Site in Protein Kinase C. *J. Med. Chem.* **1996**, *39*, 2541−2553.
(17) Nacro, K.; Bienfait, B., Lee, J.; Han, K. C.; Kang, J. H.; Benzaria, S.; Lewin, N. E.; Bhattacharyya, D. K.; Blumberg, P. M.; Marquez, V. E. Conformationally Constrained Analogues of Diacylglycerol (DAG). 16. How Much Structural Complexity Is Necessary for Recognition and High Binding Affinity to Protein Kinase C? *J. Med. Chem*. **2000**, *43*, 921−944.
(18) Roaten, J. B.; Kazanietz, M. G.; Sweatman, T. W.; Lothstein, L.; Israel, M.; Parrill, A. L. Molecular Models of N-Benzyladriamycin-14-valarate (AD 198) in Complex with the Phorbol Ester-Binding C1b Domain of Protein Kinase C-ò. *J. Med. Chem.* **2001**, *44*, 1028−1034.
(19) Pak, Y.; Enyedy, I. J.; Varady, J.; Kung, J. W.; Lorenzo, P. S.; Blumberg, P. M.; Wang, S. Structural Basis of Binding of High-Af_nity Ligands to Protein Kinase C: Prediction of the Binding Modes through a New Molecular Dynamics Method and Evaluation by Site-Directed Mutagenesis. *J. Med. Chem.* **2001**, *44*, 1690−1701.
(20) Newton, A. C.; Johnson, J. E. Regulation of Protein Kinase C by Two Membrane-Targetting Domains. *Biochim. Biophys. Acta Biomembr.* **1998**, *1376*, 155−172.
(21) Johnson, J. E.; Giorgione, J.; Newton, A. C. The C1 and C2 Domains of Protein Kinase C are Independent Membrane Targeting Modules, with Specificity for Phosphatidylserine Conferred by the C1 Domain. *Biochemistry* **2000**, *39*, 11360−11369.
(22) Mosior, M.; Newton, A. C. Calcium-Independent Binding to Interfacial Phorbol Esters Causes Protein Kinase C to Associate with Membranes in the Absence of Acidic Lipids. *Biochemistry* **1996**, *35*, 1612−1623.
(23) Mosior, M.; Newton, A. C. Mechanism of Interaction of Protein Kinase C with Phorbol Esters: Reversibility and Nature of Membrane Association. *J. Biol. Chem.* **1995**, *270*, 25526−25533.
(24) Pandit, S. A.; Berkowitz, M. L. Molecular dynamics simulation of dipalmitoylphosphatidylserine bilayer with Na^+ counterions. *Biophys. J.* **2002**, *82*, 1818−1827.
(25) Mukhopadhyay, P.; Monticelli, L.; Tieleman, D. P. Molecular Dynamics Simulation of a Palmitoyl-Oleoyl Phosphatidylserine Bilayer with Na^+ Counterions and NaCl. *Biophys. J.* **2004**, *86*, 1601−1609.
(26) Bond, P.; Sansom, M. S. P. Membrane Protein Dynamics versus Environment: Simulations of OmpA in a Micelle and in a Bilayer. *J. Mol. Biol.* **2003**, *329*, 1035−1053.
(27) Kothekar, V. 260 ps Molecular Dynamics Simulation of Substance P with Hydrated Dimyristolyl Phosphatidyl Choline Bilayer. *J. Biom. Struct. Dyn.* **1996**, *13*, 601−613.
(28) Tieleman, D. P.; Berendsen, H. J. C. A molecular dynamics study of the pores formed by *Escherichia coli* OmpF porin in a fully hydrated palmitoyloleoylphosphatidylcholine bilayer. *Biophys. J.* **1998**, *74*, 2786−2801.
(29) Berneche, S.; Roux, B. Molecular dynamics of the KcsA Kp channel in a bilayer membrane. *Biophys. J.* **2000**, *78*, 2900−2917.
(30) Gullingsrud, J.; Kosztin, D.; Schulten, K. Structural determinants of MscL gating studied by molecular dynamics simulations. *Biophys. J*. **2001**, *80*, 2074−2081.
(31) Jensen, M. Ø.; Tajkhorshid, E.; Schulten, K. The mechanism of glycerol conduction in aquaglyceroporins. *Structure* **2001**, *9*, 1083−1093.
(32) Sansom, M. S. P.; Shrivastava, I. H.; Ranatunga, K. M.; Smith, G. R. Simulations of ion channels—watching ions and water move. *Trends Biochem. Sci*. **2000**, *25*, 368−374.
(33) Berman, H. M.; Westbrook, J.; Feng, Z.; Gilliland, G.; Bhat, T. N.; Weissig, H.; Shindyalov, I. N.; Bourne, P. E. The Protein Data Bank. *Nucleic Acids Res.* **2000**, *28*, 235−242.
(34) Quest, A. F. G.; Bardes, E. S. G.; Bell, R. M. A Phorbol Ester Binding Domain of Protein Kinase Cγ. Deletion Analysis of the Cys2 Domain Defines a Minimal 43-Amino Acid Peptide. *J. Biol. Chem.* **1994**, *269*, 2961−2970.
(35) Hermans, J.; Berendsen, H. J. C.; van Gunsteren, W. F.; Postma, J. P. M. A Consistent Empirical Potential for Water−Protein Interactions. *Biopolymers* **1984**, *23*, 1513−1518.
(36) van Gunsteren, W. F., Berendsen, H. J. C. Gromos-87 Manual, Biomos BV: Groningen, 1987.
(37) Berendsen, H. J. C.; van der Spoel, D.; van Drunen, R. GROMACS: A Message-Passing Parallel Molecular Dynamics Implementation. *Comput. Phys. Commun.* **1995**, *95*, 43−56.
(38) Lindahl, E.; Hess, B.; van der Spoel, D. Gromacs 3.0: A Package for Molecular Simulation and Trajectory Analysis. *J. Mol. Mod.* **2001**, *7*, 306−317.
(39) Berendsen, H. J. C.; Postma, J. P. M.; van Gunsteren, W. F.; Hermans, J. Interaction Models for Water in Relation to Protein Hydratation. In *Intermolecular Forces.* Pullman, B., Ed.; D. Reidel Publishing Co.: Dordrecht, 1981, pp 331−342.
(40) Lindahl, E.; Edholm, O. Mesoscopic Undulations and Thickness Fluctuations in Lipid Bilayers from Molecular Dynamics Simulations. *Biophys. J.* **2000**, 79, 426−433.
(41) Berger, O.; Edholm, O.; Jähnig, F. Molecular Dynamics Simulation of a Fluid Bilayer of Dipalmitoylphosphatidylcholine at Full Hydration, Constant Pressure and Constant Temperature. *Biophys. J.* **1997**, *72*, 2002−2013.
(42) Nagle, J. F.; Wiener, M. C. Structure of Fully Hydrated Bilayer Dispersions. *Biochim. Biophys. Acta.* **1988**, *942*, 1−10.
(43) Seelig, J.; Seelig, A. Dynamic Structure of Fatty Acyl Chains in a Phospholipid Bilayer Measured by NMR. *Biochemistry.* **1974**, *13*, 4839−4845.
(44) Chiu, S.; Clark, M.; Balaji, V.; Subramaniam, S.; Scott, H.; Jakobsson, E. Incorporation of Surface Tension into Molecular Dynamics Simulation of an Interface: A Fluid Phase Lipid Bilayer Membrane. *Biophys. J.* **1995**, *69*, 1230−1245.
(45) Jorgensen, W.; Tirado-Rives, J. The OPLS Potential Functions for Proteins. Energy Minimizations for Crystals of Cyclic Peptides and Crambin. *J. Am. Chem. Soc.* **1988**, *110*, 1657−1666.
(46) Ryckaert, J. P.; Ciccotti, G.; Berendsen, H. J. C. Numerical Integration of the Cartesian Equations of Motion of a System with Constraints; Molecular Dynamics of *n*-Alkanes. *J. Comput. Phys.* **1977**, *23*, 327−341.
(47) Verlet, L. Computer "Experiments" on Classical Fluids. I. Thermodynamical Properties of Lennard-Jones Molecules. *Phys. Rev.* **1967**, *159*, 98−103.
(48) Hess, B.; Bekker, H.; Berendsen, H. J. C.; Fraaije, J. G. E. M. LINCS: A Linear Constraint Solver for Molecular Simulations. *J. Comput. Chem.* **1997**, *18*, 1463−1472.
(49) Miyamoto, S.; Kollman, P. A. J. Settle—An Analytical Version of the Shake and Rattle Algorithm for Rigid Water Models. *Comput. Chem.* **1992**, *13*, 952−962.
(50) Berendsen, H. J. C.; Postma, J. P. M.; DiNola, A.; Haak, J. R. Molecular Dynamics with Coupling to an External Bath. *J. Chem. Phys.* **1984**, *81*, 3684−3690.
(51) Essmann, U.; Perera, L.; Berkowitz, L. A. Smooth Particle Mesh Ewald Methodology. *J. Chem. Phys.* **1995**, *103*, 8577−8593.
(52) Humphrey, W.; Dalke, A.; Schulten, K. VMD − Visual Molecular Dynamics. *J. Mol. Graphics* **1996**, *14*, 33−38.
(53) The POV−Ray program was obtained from http://www.povray.org.
(54) Kabsch, W.; Sander, C. Dictionary of Protein Secondary Structure: Pattern Recognition of Hydrogen-Bonded and Geometrical Features. *Biopolymers* **1983**, *22*, 2577−2637.
(55) Sugita, K.; Neville, Ch. F.; Sodeoka, M.; Sasai, H., Shibasaki M. Stereocontrolled Syntheses of Phorbol Analogues and Evaluation of their Binding Affinity to PKC. *Tetrahedron Lett.* **1995**, *36*, 1067−1070.
(56) Sodeoka, M.; Uotsu, K.; Shibasaki M. Photoaffinity Labeling of PKC with a Phorbol Derivative: Importance of the 13-Acyl Group in Phorbol Ester-PKC interaction. *Tetrahedron Lett.* **1995**, *36*, 8795−8798.
(57) Tanaka, M.; Irie, K.; Nakagawa, Y.; Nakamura, Y.; Ohigashi, H.; Wender, P. A. The C4 Hydroxyl Group of Phorbol Esters Is Not Necessary for Protein Kinase C Binding. *Bioorg. Med. Chem. Lett.* **2001**, *11*, 719−722.

JM049786S